APPLICATIONS OF CALCIUM SILICATES DERIVED FROM GEOTHERMAL RESOURCES

Mathew J. Cairns[1], James H. Johnston[1], Thomas Borrmann[1], H. Putri Fraser[1] and Michael Schweig[1]

[1] School of Chemical and Physical Sciences, Victoria University of Wellington, PO Box 600, Wellington 6140, New Zealand

mathew.cairns@vuw.ac.nz

Keywords: *Nano-structured calcium silicate, silica scale, cement.*

ABSTRACT

We have developed a process to remove dissolved silica from geothermal brines in the form of a proprietary calcium silicate hydrate material (CaSil). By decreasing the level of dissolved silica in the brine below the silica saturation index, we can effectively reduce the formation of intractable silica sinter within pipework and associated equipment. The formed CaSil material does not adhere to pipework and can be recovered from solution, allowing the brine to be reinjected without risk of silica deposition in the reinjection well.

The recovered calcium silicate has a low bulk density and a high surface area, with the calcium component of the CaSil remaining chemically available. These properties make the CaSil amenable to incorporation into concrete materials based on Portland cement. The CaSil/cement composite materials are lightweight and have the potential to be used as construction materials.

This paper will discuss the properties of the composite materials and their potential uses.

1. INTRODUCTION

Hot geothermal fluids in underground reservoirs usually contain high concentrations of dissolved minerals, which in general have higher solubility at elevated temperature (above 200 °C). When these fluids are extracted from the reservoir and utilized for direct steam geothermal power generation, both the temperature and volume of the liquid phase of the brine are decreased during the steam flashing process. This can cause some dissolved minerals in the liquid phase to reach supersaturated concentration levels. These supersaturated minerals, particularly silica, can precipitate from the brine phase. In the case of silica, this can lead to the formation of a hard, intractable scale material, which can restrict fluid flow through equipment such as pipework, heat exchangers and reinjection wells, negatively impacting the operational efficiency of the system (Zarrouk et al. 2014).

In general, the precipitation of dissolved minerals can be minimized by operating steam-flash vessels or heat exchangers at a higher brine outlet temperatures. However, this has thermodynamic disadvantages, as less useful energy can be extracted from the geothermal fluid. Dissolved silica usually exists in freshly extracted hot brine as silicic acid, or one of its deprotonated forms, e.g. $H_3SiO_4^-$. Careful control of the pH levels of the brine can delay the onset of the precipitation reactions (Gallup 2011). Alternatively, other additives such as alkoxide or phosphonate polymers may be used to inhibit the polymerization of silica or precipitation of calcite (Gill 2011). A disadvantage of these techniques is that the scale-forming species are not removed from the brine. If the brine chemistry is not carefully controlled and monitored, scale formation can still occur.

Once scale is formed, its removal from equipment such as heat exchangers is a labour-intensive process (Zarrouk et al. 2014). As such, controlling silica scale can impose a large economic burden on the operation of geothermal energy systems.

We have developed a method by which dissolved silica in geothermal brines can be converted to a nano-structured calcium silicate hydrate material (CaSil) via the addition of a suitable calcium source to the geothermal brine under basic pH conditions (Johnston et al. 2006, Borrmann and Johnston, 2017). Overall, the reaction proceeds according to the simplified reaction:

$$H_3SiO_4^- + Ca^{2+} + xOH^- \rightarrow CaSiO_{3-x}(OH)_{2x}.yH_2O$$

The reaction between the calcium and the dissolved silica can be controlled to either remove all dissolved silica from the brine, or to simply reduce the dissolved silica concentration to below the saturation level at a given temperature. Unlike silica, the formed CaSil material does not adhere to metal surfaces, meaning intractable silica or silica-like scale is no longer formed within the system. This has direct thermodynamic advantages in that heat exchangers or similar may be operated at a lower outlet temperature without causing scale formation, enabling more energy to be extracted from the geothermal brine. The CaSil material may also be separated and removed from the brine phase with high efficiency. We have been operating a pilot plant demonstrating this technology at the Wairakei geothermal field, New Zealand, since 2017 (Borrmann and Johnston 2017). The primary aim of the pilot plant operation is to prevent silica scale within geothermal equipment. However, the separated calcium silicate material has several useful properties and potential applications. The typical morphology of the CaSil material obtained from the pilot plant operation is shown by the scanning electron micrograph provided in Figure 1.

The CaSil material consists of interlinked platelets forming particles a few microns in size. This imparts a high surface area of 200 – 400 $m^2\ g^{-1}$, depending on preparation conditions. The particles will readily form loose flocs, which enable low-cost, small footprint techniques such as lamella separation to be employed for its efficient removal from geothermal brine (Schweig et al. 2018). Upon standing, a suspension of CaSil will settle to form a material containing 2 – 5 wt% solids, with the other 95 – 98 wt% comprising water. Vacuum filtration can be used to further increase the solids content, but typically a filter-cake of CaSil still comprises 80 – 95 wt% water. The CaSil material in this form is thixotropic, such that modest mechanical mixing is sufficient to re-disperse the material to its fundamental micron-sized particles. Ideally, the CaSil would be used in the form of a filter-cake, as this preserves the small particle

size and high surface area. Fully removing all water from the CaSil requires heating, an energy-intensive process. When dried, the CaSil prepared from geothermal brine forms a friable powder, and can re-adsorb 250% of its mass as water, before becoming saturated. However, when the CaSil is prepared under certain synthetic conditions, the material can agglomerate upon drying, with a corresponding loss of pore volume and surface area (Johnston et al. 2006).

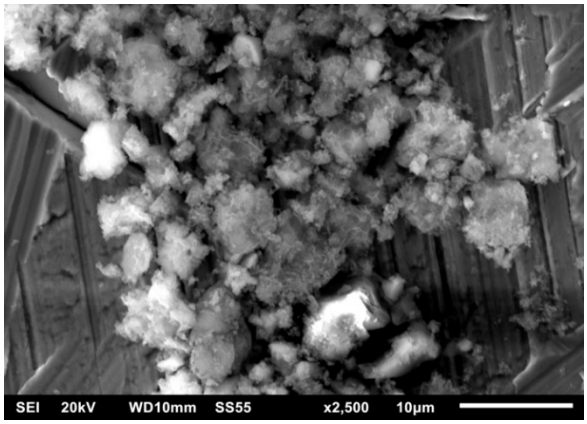

Figure 1: Scanning electron micrograph of CaSil material recovered from pilot-plant operations.

We have previously prepared this CaSil material from synthetic silica sources such as aqueous sodium silicate (Johnston et al. 2006). Previous applications of this material include exploiting the high surface area of the material as an additive in paper coating to improve print quality (Mesic and Johnston 2013). Alternatively, the CaSil has been used as an adsorbent for phosphate (Cairns and Borrmann 2014) or heavy metal ions (Borrmann et al. 2011). This application exploits the high pH of the CaSil surface and the chemical activity of the calcium component of the material to precipitate calcium phosphate or metal hydroxide species.

One further potential use of the CaSil which exploits the chemical activity of the calcium component is as an additive in cement and concrete materials. Portland cement is one of the most widely utilized cements in the construction industry. The major component of cement is tricalcium silicate, Ca_3SiO_5, with tricalcium aluminate, silica and calcium sulfate usually also present. Ca_3SiO_5 reacts with water according to:

$$Ca_3SiO_5 + H_2O \rightarrow 3Ca^{2+} + H_2SiO_4^{2-} + 4OH^-$$

Over time, as the cement sets, calcium silicate hydrate and calcium hydroxide phases are formed. The reactions occurring during cement hydration and setting are complex – Bullard et al. (2011) provide a review of the subject. However, as cement forms calcium silicate hydrate phases during curing, it is potentially chemically compatible with the CaSil product we obtain from geothermal brines. We have investigated this by preparing composites of Portland cement and CaSil.

2. METHODS

Samples of calcium silicate hydrate were obtained from the pilot plant located at Wairakei, New Zealand as described by Borrmann and Johnston (2017). Alternatively, synthetic samples of CaSil were prepared according to the method described by Johnston et al. (2006). For both silicate materials, samples were vacuum filtered to provide a filter cake containing typically 5 – 10 wt% solids (dry basis at 120 °C). The CaSil filter cake exhibits thixotropic behaviour and can be re-dispersed to form a slurry with the application of mechanical agitation.

In some cases, the entirety of the filter cake material was dried, and subsequently ground to a fine powder before use.

Composites of calcium silicate and cement were prepared by dispersing the calcium silicate, ordinary Portland cement and water with a mechanical mixer for 15 minutes before being cast into shallow moulds (10 mm depth). Moulds were agitated during packing to prevent the inclusion of large air voids. Filled moulds were sealed with plastic film and cured at 20 °C for 48 hours. When dried calcium silicate material was used, this was dispersed with the dry cement component prior to addition of water. If calcium silicate filter cake was used, this was re-dispersed to a slurry within the mixer prior to the addition of cement. No other aggregates such as sand or gravel were added to the mixtures. In the case of no CaSil addition, a water: cement mass ratio of 0.4:1 was chosen. In other cases, sufficient additional water was added to overcome the 250 wt% water adsorption capacity of the dried CaSil.

Sample density and porosity were measured of monolithic samples after removal from the moulds and drying to constant mass at 60 °C. Porosity was calculated as the volume of water adsorbed by a monolithic sample of known volume. Dry-basis CaSil content was calculated according to the mass of dry materials (cement and dry CaSil powder) added to the composite. In cases where CaSil filter-cake was used, the known solids content of the filter-cake was used to provide a dry-equivalent mass of CaSil for the calculation.

Powder X-ray diffraction (XRD) measurements were collected with a Panalytical MPD X'Pert Pro diffractometer utilizing a Cu Kα radiation source. Microscopic analysis of samples was undertaken with a JEOL JSM 6100LA scanning electron microscope. Cured CaSil-cement composites were fractured to provide segments for analysis of ca. 2 mm x 5 mm x 5 mm in size. Dried CaSil was analysed as a fine powder. Scanning electron micrographs (SEM) were captured either as secondary electron (SEI) or composite backscattered electron (BEC) images.

3. RESULTS AND DISCUSSION

Composites of CaSil and cement were prepared from geothermal CaSil, either in filter-cake form or as dried solids, with the data given in Figure 2. From the figure, it can be seen that the composites exhibit a decrease in monolithic density and an increase in porosity with increased CaSil content. When a comparison is made between the composites prepared from CaSil filter cake and dry CaSil, it can be seen that for a given CaSil content of the composite, the density is lower if that composite was prepared from CaSil filter cake than from dry CaSil powder. The range of CaSil content presented in Figure 2 covers the range for which the set composites retained structural integrity. When the CaSil content was increased above ca. 35 wt%, the set composites became friable, similar to the behaviour of dried CaSil itself.

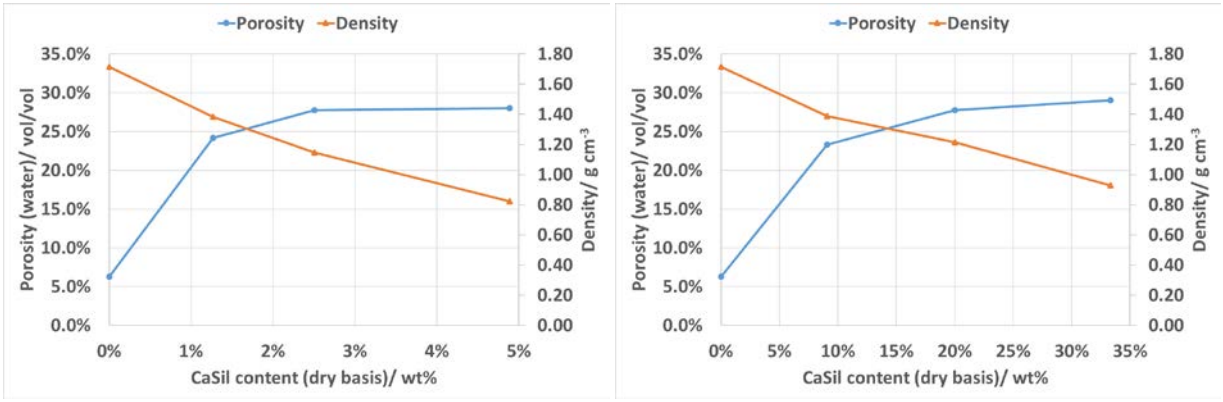

Figure 2: Porosity and density of CaSil/cement composites prepared with geothermal CaSil filter-cake (a) or dried geothermal CaSil (b).

Given the observation that the composites provided lower density when prepared with CaSil filter cake, rather than dry CaSil, the density of the set samples was compared to the water content of the slurry when cast. This data is given in Figure 3, which includes composites prepared from both geothermal and synthetic CaSil, either as the filter-cake or dry powder form. A clear trend is observed in that the bulk density of the set composites decreases with an increased water content used in its preparation. Only minor changes are observed between the density of samples prepared from synthetic and geothermal CaSil materials.

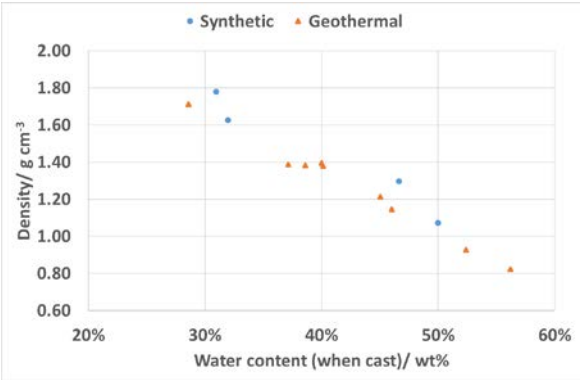

Figure 3: Density of composites of CaSil and cement prepared from either synthetic or geothermal CaSil.

The powder X-ray diffraction patterns of composites prepared from synthetic CaSil and cement are presented in Figure 4a. Diffraction patterns of samples containing only hydrated cement or dried CaSil are also provided in the figure as the 0% and 100% traces respectively. In the CaSil material, the primary crystalline phase present is calcite, $CaCO_3$. For the hydrated cement, the primary crystalline phase is lime, $Ca(OH)_2$. Major reflections in the diffraction patterns of these compounds have been indicated in the figure by circular or triangular points. A semi-quantitative analysis of these two phases was plotted as a function of CaSil present in the composite, with the data given in Figure4b. The semi-quantitative phase analysis data shows a linear increase in the $CaCO_3$ content with increasing CaSil content, up to 50 wt% CaSil in the dry composite. A corresponding decrease in the $Ca(OH)_2$ content is observed with an increase in CaSil content. The linear relationship between the phase composition and the CaSil content indicates that the presence of CaSil does not significantly alter the nature of the products formed during the cement hydration reactions. Above 50% CaSil content, the semi-quantitative phase analysis remains stable at ca. 90% $CaCO_3$ and ca. 10 % $CaOH_2$. Small residual $Ca(OH)_2$ quantities present even at high CaSil content are likely an artefact of the semi-quantitative analysis, due to the presence of some overlapping reflections in the $CaCO_3$ and $Ca(OH)_2$ diffraction patterns.

Other than the reflections associated with the major $CaCO_3$ or $Ca(OH)_2$ phases, most minor reflections present in the XRD pattern of the composite materials were also present in the hydrated cement sample.

Typical SEM images of the composite materials are provided in Figure 5. An image of a CaSil-free hydrated cement material is provided in 5a. The image shows a dense material with firmly embedded crystallites of 10 – 50 µm in size. The large crack present at the left of the image is an artefact of the fracturing technique used to prepare samples for SEM analysis. Few other voids are present in this sample.

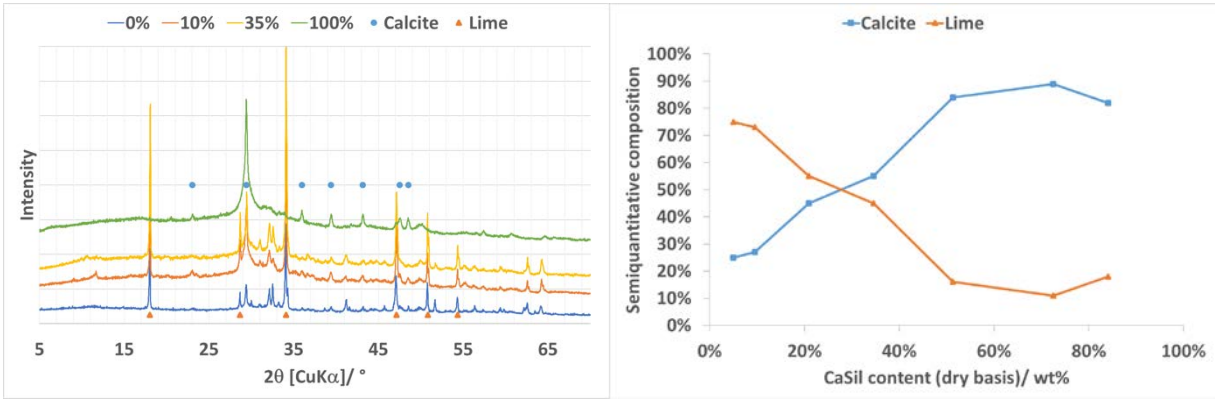

(a) **(b)**

Figure 4: Representative powder XRD patterns of composites prepared from synthetic CaSil filter-cake (a) and semi-quantitative $Ca(OH)_2$ or $CaCO_3$ content of composite (b). Representative reflections of calcite [$CaCO_3$] and lime [$Ca(OH)_2$] are provided in (a). Figure legend of (a) indicates dry CaSil content of the composite material (wt%).

By contrast, a sample containing 9 wt% geothermal CaSil is provided in Figure 5b. Large voids of up to 100 µm in size are present in this sample, which are not otherwise present in the CaSil-free sample. This is consistent with the data presented in Figure 2, which shows a large increase in sample porosity when CaSil is present in the composites.

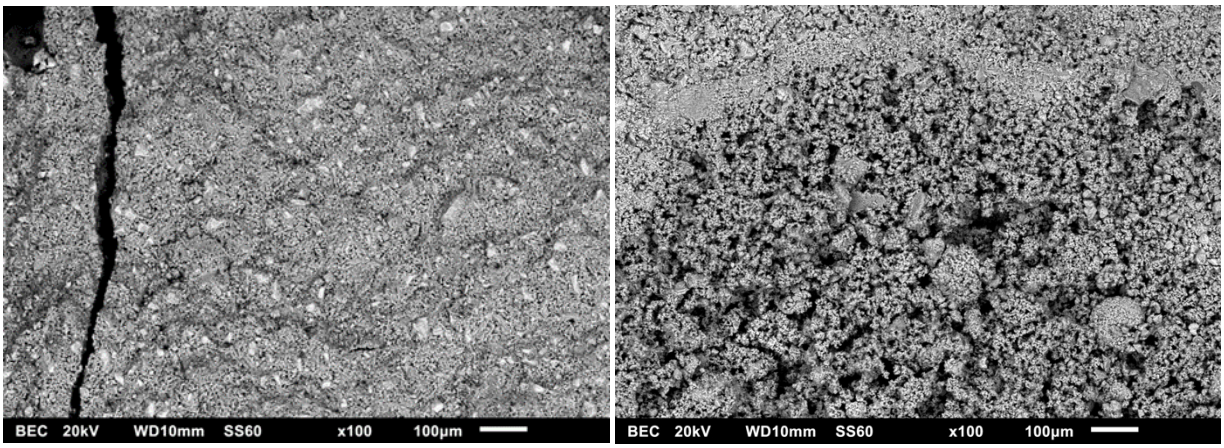

(a) **(b)**

Figure 5: Representative SEM images of composites of CaSil and cement: hydrated cement only (a); geothermal CaSil and hydrated cement showing increased porosity (b). Images captured in composite backscattered electron scanning mode.

Higher-magnification images of these samples are provided in Figure 6. The CaSil material in the sample shown in Figure 6b is present as amorphous powder throughout the sample. Needle-like material can be seen growing from the CaSil material, as indicated by the red box in Figure 6b. These needle-like structures are not present in the CaSil-free hydrated cement sample, Figure 6a. From the XRD data presented in Figure 4a, most crystalline phases present in the CaSil-cement composites, other than $CaCO_3$ are also present in the CaSil-free hydrated cement sample. This indicates that the needle-like material present in Figure 6b is either $CaCO_3$, or otherwise very similar to a cement hydration product. This is also evidence for the CaSil being chemically active during the cement hydration reactions, rather than simply acting as a chemically inert aggregate material.

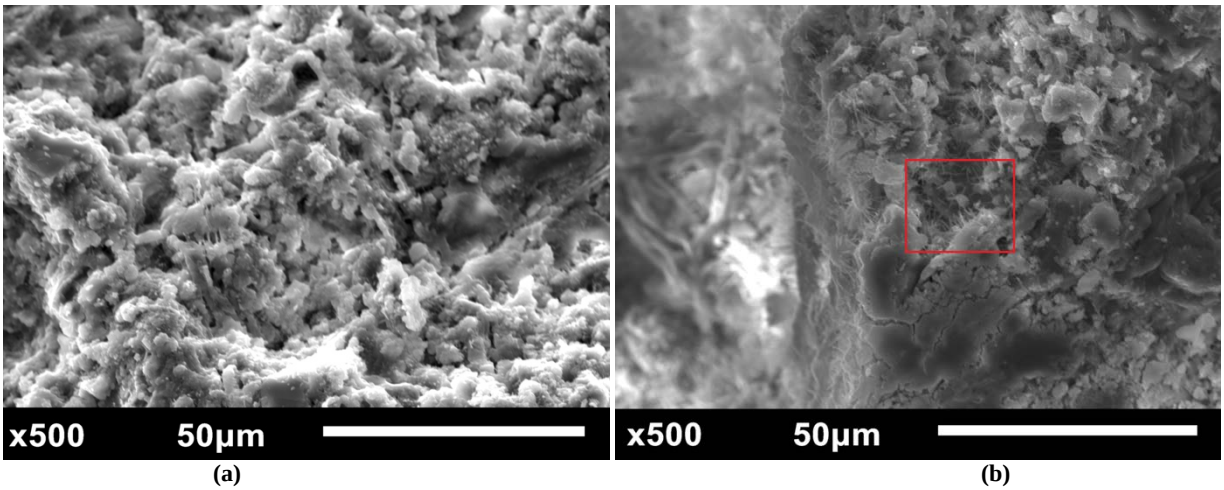

(a) (b)

Figure 6: Representative SEM images of composites of CaSil and cement: hydrated cement only (a); geothermal CaSil and hydrated cement showing growth of needle-like material from CaSil present in sample (b). Images captured in secondary electron imaging mode.

From the SEM images presented in Figure 5, the voids present in the CaSil-containing samples are significantly larger than the void volume present within individual CaSil particles (Figure 1). As such, it is unlikely that the high surface area of CaSil contributes directly to the high porosity of the composite materials. Rather, it is likely that the large voids in the sample are a result of water evaporation during sample curing. This is consistent with the data from Figure 3, which shows a decrease of sample density with an increase of water content in the samples when cast. The high water adsorption capacity and thixotropic behaviour of CaSil is beneficial in this context, as it enables samples to be cast at higher water content than CaSil free cement.

4. CONCLUSIONS

We have demonstrated the incorporation of a calcium silicate hydrate material into cement composite materials. The CaSil material exhibits chemical compatibility with the cement, showing evidence of chemical reaction during the curing process. CaSil formed no unexpected crystalline phases during cement hydration. The composite materials themselves provide a much lower bulk density and higher porosity than the unmodified cement material.

It is expected that the low density and high porosity of the composite materials would provide for reduced thermal conductivity, which makes them interesting for applications such as light-weight and flame-retardant wall panels. The low thermal conductivity is already a known property of the CaSil material, which provides a thermal conductivity of approximately 0.03 W m^{-1} K^{-1} due to the low bulk density and high pore volume of the unmodified material (Johnston et al. 2006). The thermal behaviour of these composite materials will be reported at a later date.

ACKNOWLEDGEMENTS

This project has been funded by the New Zealand Ministry of Business, Innovation and Employment Research Grant RTVU1604. We would also like to thank MB Century Ltd. and the Tuaropaki Trust, Wairakei, New Zealand, especially Marcel Manders and Richard Adams for their collaboration and support in providing access to geothermal water resources and facilities.

REFERENCES

Borrmann, T., Cairns, M. J., and Anderson, B. G.: Nano-Structured Calcium Silicate as Sorbent in a Study of Artificial Mining Waste, *International Journal of Environment and Waste Management*, 8, pp. 383 – 403, (2011).

Borrmann, T., and Johnston, J. H., Transforming Silica into Silicate – Pilot Scale Removal of Problematic Silica from Geothermal Brine, *GRC Transactions*, 41, pp. 1322 – 1333, (2017).

Bullard, J. W., Jennings, H. M., Livingston, R. A., Nonat, A., Scherer, G. W., Schweitzer, J. S., Scrivener, K. L., Thomas, J. J., Mechanisms of Cement Hydration, *Cement and Concrete Research*, 41, pp. 1208 – 1223, (2011).

Cairns, M. J., and Borrmann, T.: Batch and Continuous Phosphate Uptake Studies Employing a Ferrimagnetic Calcium Silicate Hydrate Composite, *RSC Advances*, 4, pp. 53475 – 53483, (2014).

Gallup, D.L., pH Modification Scale Control Technology, *Proceedings*, International Workshop on Mineral Scaling, Manila, Philippines, 25-27 May, (2011), 39 – 46.

Gill, J.S., New Inhibitors for Silica and Calcium Carbonate Control in Geothermal, *Proceedings*, International Workshop on Mineral Scaling, Manila, Philippines, 25-27 May, pp. 113 – 118, (2011).

Johnston, J. H., Borrmann, T., and McFarlane, A. J.: Nano-structured Calcium Silicate, Functionalised Forms Thereof, Preparation and Uses, *NZ Patent Specification* No 537747 (2006).

Mesic, B., and Johnston, J. H.: Inkjet Printability of Newsprint: Effects of Starch-based Coatings, *TAGA Journal of Graphic Technology*, 6, 18 – 37, (2013).

Schweig, M., Johnston, J. H., Borrmann, T., and Cairns, M. J.: Lamella Separators for Recovering Nano-Structured Calcium Silicate Hydrate from Geothermal Brine, *GRC Transactions*, 42, 1240 – 1250, (2018).

Zarrouk, S. J., Woodhurst, B. C., and Morris, C.: Silica Scaling in Geothermal Heat Exchangers and its Impact on Pressure Drop and Performance: Wairakei Binary Plant, New Zealand, *Geothermics*, 51, 445 – 459, (2014).